International Journal of Thin Film Science and Technology

Volume 1
Issue 1 *May 2012*

Article 3

2012

Investigation on high carrier mobility in chromium incorporated CdO thin films on glass

A. A. Dakhel
Universiy of Bahrain, adakhil@sci.uob.bh

International Journal of Thin Films Science and Technology
An International Journal

Investigation on high carrier mobility in chromium incorporated CdO thin films on glass

A. A. Dakhel[(1)] and H. Hamad [(2)]
(1) *Department of Physics, College of Science, University of Bahrain, P.O. Box 32038, Kingdom of Bahrain.*
(2) *University of Abu Dhabi P.O. Box 59911, United Arab Emirates.*
Email: adakhil@sci.uob.bh

Received: Jan. 11, 2012; Revised March 4, 2012; Accepted April 17 6, 2012
Published online: 1 May 2012

Abstract: Several sets of CdO thin films doped with different amount of chromium have been grown on glass substrates by a vacuum evaporation technique. The effects of Cr doping on the structural, electrical, and optical properties of the host CdO films were systematically studied. The X-ray diffraction study shows that some of Cr ions occupied locations in interstitial positions and/or Cd-ion vacancies in CdO lattice. The bandgap of Cr-doped CdO suffer variations that were studied in the framework of the available models based on simultaneous effects of bandgap widening and bandgap narrowing. The electrical behaviours show that all the prepared Cr-doped CdO films are degenerate semiconductors. However, the Cr doping influences all the optoelectrical properties of CdO. Their dc-conductivity carrier concentration and mobility increase with small 1-1.8% Cr-incorporation level compare to undoped CdO film. The largest mobility (85.2 $cm^2/V.s$) and conductivity (2150 S/cm) were measured with 1.3%Cr. From near infrared-transparent-conducting-oxide (NIR-TCO) point of view, Cr is effective for CdO slight doping.

Keywords: Cadmium-boron oxide; boron-doped CdO; CdO

1 Introduction

Transparent conduction oxides (TCO) are a type of nonstoichiometric semiconductor oxides of high conductivity arising from structural metal interstitials and oxygen vacancies. They have widespread use in many advanced technology applications. It is essential to investigate means for improving the function of TCOs since they could have an enormous impact on the next generation flat panel displays and solar energy systems, and any progress in this field will require a dedicated, multidisciplinary effort [1]. It is well known that high carrier mobility (μ_{el}) is essential for TCOs with good quality electro-optical properties. From other side sometimes it is necessary to hybridize TCO in order to get some magnetic or other properties for various applications. The hybridization can be realized by doping with elements having the required wanted property to be appeared in the TCO.

One of the known TCOs, CdO is the subject of the present study as doped with chromium. Chromium is remarkable for its antiferromagnetic magnetic properties at and below room temperature. Furthermore, chromium has a high corrosion resistance and hardness like adding to steel to form stainless steel. CdO is a degenerate n-type semiconductor with electrical conductivity $10^2 - 10^4$ $S\,cm^{-1}$ and transparent in visible and NIR spectral regions with a direct bandgap of 2.2 - 2.7 eV [2-4]. The n-type electrical conduction in CdO is due to Cd interstitial (Cd_i) and oxygen vacancies (V_O), however the V_O is dominate defect acting as doubly ionized (+2) charge shallow donors [4].

The objective of the present investigation is to control the electronic mobility in CdO by Cr incorporation. It was observed [5] that the carrier mobility in a grown CdO films significantly depends on the type of the substrate and its temperature for example, CdO film grown on glass substrate at 412 ^oC shows high room-temperature mobility (105 $cm^2/V.s$) while it was 307 $cm^2/V.s$ for that film grown on single-crystal MgO at 400 ^oC. These results were explained by the different in scattering of carriers by neutral impurity (NIS) rather than ionized impurity or grain boundaries i.e. increased mobilities is attributed to a reduction in NIS caused by improved crystallinity in several cases. Coutts et al. [6] have prepared CdO film on glass substrate with mobility 200 $cm^2/V.s$. Furthermore, the carrier mobility as one

of the optoelectronic properties of CdO could be controlled by doping with different metallic ions [2,7-10]. It was observed that dopant ions of slightly smaller size than that of Cd^{2+} could improve the electronic conductivity and mobility. However, doping by using any technique of CdO with ions of much smaller radius like chromium has not yet been investigated, although such doping was conducted for other TCO's like ZnO [11-13], SnO2 [14], and In2O3 [15,16].

The present fundamental work reports the effect of chromium doping on the structural, electrical, optical, and optoelectronic properties of CdO. It will be seen that chromium doping of CdO is efficient in construction electronic transport ways for obtaining high mobility in comparison with other dopants and could be successfully used for technical applications based on its IR-TCO characteristics.

2. Experimental details

Ten sets of CdO thin films doped with different amount of chromium were grown on glass and silicon substrates. The starting materials, pure Cr and CdO (from Fisher sci. company/USA and Fluka A.G./Germany, respectively) were evaporated alternatively (layer-by-layer) by alumina baskets (Midwest tungsten service, USA). The substrates were ultrasonically clean glass slides and chemically (using HF) cleaned silicon wafer held in a vacuum chamber of residual oxygen atmosphere of about 1.3×10^{-3} Pa. The as-grown films were totally oxidized and stabilized by flash annealing in air at 400 ^{o}C for 1 h keeping samples inside the closed furnace for slow natural cooling to room temperature. All samples were prepared in almost the same conditions including the reference pure CdO film. The evaporated masses were controlled with a piezoelectric microbalance crystal sensor of a Philips FTM5 thickness monitor fixed close to the substrate. The thicknesses were measured after annealing by an MP100-M spectrometer (Mission Peak Optics Inc., USA), to be 0.12-0.25 μm. The structures of the prepared films were studied with X-ray diffraction (XRD) method using a Philips PW 1710 θ□-2θ system with a Cu K_α radiation (0.15406 nm) and a step of 0.02^{o}. The energy dispersion X-ray fluorescence (EDXRF) method was used to determine the relative weight ratio Cr to Cd (r) in the studied films. The spectral optical transmittance T(λ) was measured at normal incidence in UV-VIS-NIR spectral region (300 - 3000 nm) with a Shimadzu UV-3600 double beam spectrophotometer. The electrical measurements were carried out with a standard Van-der-Pauw method with aluminum dot contacts in a magnetic field of about one Tesla and using a Keithley 195A digital multimeter and a Keithley 225 current source.

3. Results and discussion

3.1. Structural characterization

The energy-dispersive X-ray fluorescent (EDXRF) method was used to determine the Cr content in each sample. Fig.1 shows the EDXRF spectrum for one of the samples. The spectrum shows Cd L-band (3.13 - 3.53 keV) and Cr K□ band (5.41 keV) with the source Cu K_α line. The ratio of the integral intensity of Cr K_α-band (I_{Cr}) to that of Cd L-band (I_{Cd}) or (I_{Cr}/I_{Cd}) was used to determine the fractional weight ratio (r) of Cr to Cd in a film sample. For that purpose, the known method of micro radiographic analysis was used [17]. The reference samples were pure Cr and CdO thin films. The results of r-values were 0.6%, 1.0%, 1.2%, 1.3%, 1.5%, 1.8%, 2.5%, 3.6%, 4.2%, and 4.8% (wt). Each sample was named according to Cr content, e.g CdO:1.5% Cr.

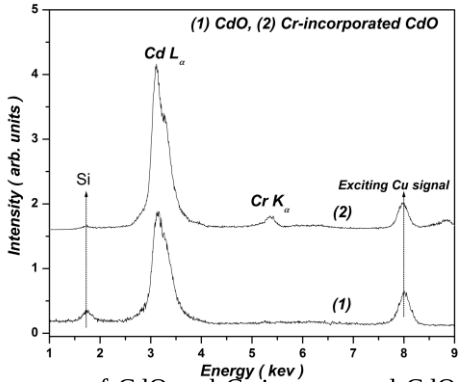

Fig.1 Energy dispersion X-ray fluorescence of CdO and Cr-incorporated CdO on Si Substrate. Cu K_α signal is the exciting energy.

Fig.2 shows the X-ray diffraction (XRD) patterns of the prepared pure and Cr-incorporated CdO films on glass substrates. These patterns reveal that all the investigated films are polycrystalline with cubic Fm3m CdO structure of a lattice constant of 0.4695 nm, as given in ref. [18]. On fig.2b, the XRD pattern of oxidized Cr film on glass substrate prepared by the same method of the present work is also shown. The Cr oxide film was at the beginning stages of crystallization. One weak peak is shown in fig.2b corresponds to Cr_2O_3 and indexed as (110) according to the known structure: Trigonal (Rhombohedral) structure ($R\,\overline{3}C$) of a= b=0.4953 nm and c=1.3578 nm, which is close to the JCPDS data [19]. There were no peaks found corresponding to Cr_2O_3 phase in the XRD patterns of Cr-doped CdO. This implies that Cr ions were dissolved in the lattice of CdO. However, for higher doping levels $r \geq 3.6\%$, some of the incorporated Cr accumulated on the crystallite and grain boundaries in form of amorphous Cr oxide, which can be discovered by optical absorption and electrical methods (next paragraphs). Several possibilities for Cr-ions to be incorporated in the host CdO crystalline lattice structure: they can occupy structural interstitial positions, occupy empty locations of Cd ions, or replace Cd ions. The actual doping by replacement of Cd^{2+} ions with Cr^{3+} ions forming substitutional solid solution (SSS) needs several conditions to be fulfilled, including the ionic-radius condition. The Shannon ionic radius [20] of Cd^{2+} is 0.095 nm for coordination number CN=6 of the CdO structure while it is 0.0615 nm for Cr^{3+} ions for the same coordination number, CN=6. Thus, the ionic-radius difference is 35%, which is much larger than 15% necessary for the formation of SSS, according to the well-known Hume-Rothery rules. Furthermore, Cr_2O_3 of crystalline structure (Rhombohedral) is different from that of CdO (cubic), which is once more, mark for the un-favorability of Cr-oxide to form a SSS with CdO. However, the close electronegativities (1.7 and 1.6 Pau for Cd and Cr respectively) support the favorability of forming SSS. Therefore, one can generally expect that Cr can be lightly doped in CdO crystalline structure. Thus, the occupation of locations in the structural interstitial positions of CdO lattice with Cr^{3+} (Cr_i) ions is most likely to happen at incorporation. Such incorporation disturbs the charge balance of the unit cell that can be settled by creation of Cd^{2+} ion vacancies (V_{Cd}) and/or formation of interstitial oxygen (O_i).

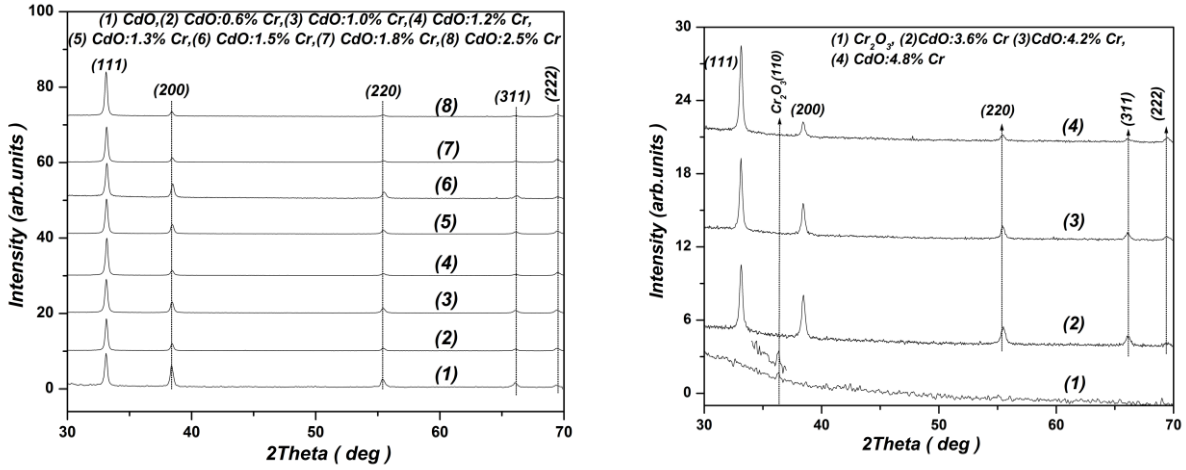

Fig.2a X-ray diffraction patterns for pure and Cr-incorporated CdO films deposited on glass substrates.
Fig.2b X-ray diffraction patterns for pure Cr_2O_3 film and Cr-incorporated CdO films deposited on glass substrates.

Some of the Cr^{3+} ions that occupy interstitial positions might move by the thermal motion, small size, and high diffusivity and occupy Cd^{2+}-ion vacancies (V_{Cd}). As mentioned in the theoretical study of Ref. [4], the O_i might move toward one of the lattice oxygens, slightly displacing it from its lattice site and forming a peroxide (O-O dumbbell-like) species, which behave like p-type defect. However, in general the O_i together with Cr accumulation on crystallite and grain boundaries reduce the effective carrier concentration and the conductivity. With this conclusive model, one can explain the electrical behavior of Cr-incorporated CdO. The entered Cr^{3+} ions in CdO lattice behave like donors while the O_i ions behave as carrier compensator or trap defects. Nevertheless, the XRD experimental accuracy did not permit to study the slight decrease in the CdO unit cell volume (v_{cell}) due to Cr incorporation.

The films grown on glass substrate have [111] preferred orientation growth, which is usual energetically preferred growth of CdO films prepared by different techniques. The mean X-ray crystallite size (CS) was estimated from the intensive (111) reflection by [21]: CS=0.9λ/βcosθ, where λ is the X-ray wavelength (0.1540 nm); β is the full-width at half maximum (FWHM) of the diffraction peak (in radian); and θ corresponds to the peak position. The CS was 35 nm for undoped CdO film that slightly decreases to 32 nm in complex manner, as shown in fig.3.

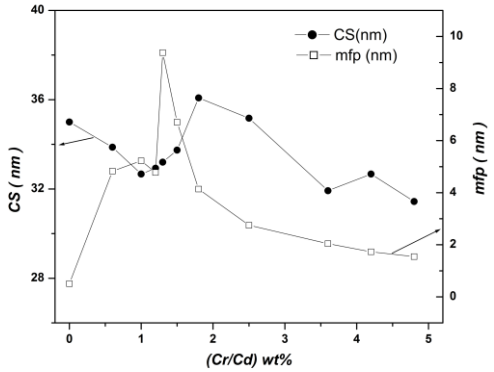

Fig.3 Variation of crystallite size (CS) and carrier mean-free-path (mfp) with Cr-incorporation% level of host CdO film grown on glass substrates.

In general, this implies that the present samples are nanocrystallites. Furthermore, the CS gives good tool to estimate the crystallinity of the film, thus the film crystallinity improves monotonically as Cr % increases between 1% and 1.8% after which it monotonically deteriorated (fig.3). The accumulation of amorphous Cd oxide on grain and crystallite boundaries can be detected with optical and electrical measurements.

3.2. DC-electrical properties

The room temperature electrical determinants [conductivity (σ), mobility (μ_{el}), and carrier concentration (N_{el})] were measured for pure and Cr-incorporated CdO films grown on glass substrates by a standard Van-der-Pauw method and the average results are presented in table 1 and fig.4. The experimental error due to the Al-contact spot size was estimated to be about 5%. The electrical measurements show that the pure and all Cr-incorporated CdO films are n-type degenerate semiconductors.

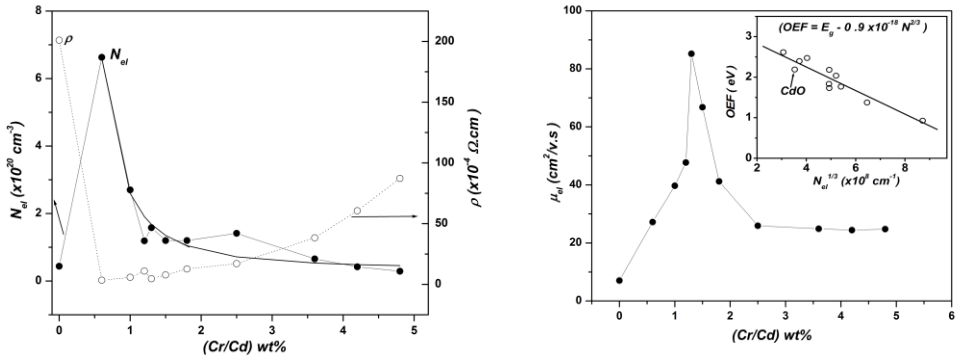

Fig.4a Variation of resistivity (ρ) and carrier concentration (N_{el}) with Cr-incorporation% level of host CdO film grown on glass substrates.

Fig.4b Variation of mobility (μ_{el}) with Cr-incorporation% level of host CdO film grown on glass substrates. The inset shows the dependence of the optoelectronic function OEF= $(E_g - S_{BGW,BGN} N_{el}^{2/3})$ on the carrier concentration $N_{el}^{1/3}$. The straight line represents the best fit according to eqn.2.

The resistivity of pure CdO thin film ($2.01x10^{-2}$ Ω.cm) was initially found to decrease rapidly to $3.46\,x\ 10^{-4}$ Ω.cm with 0.6% Cr-incorporation, then it increased slowly and monotonically with increasing of the Cr content. Similarly, the carrier concentration of pure CdO ($4.4x10^{19}$ cm^{-3}) was also found to have

initial drastic increase up to $3.63x10^{20}$ cm^{-3} then with increasing Cr incorporation it decreased strongly and monotonically. The initial rapid increase in conductivity and carrier concentration of host CdO film with a light (0.6%) addition of Cr ions indicates that most of the incorporation Cr ions act as donors. However, the increase in Cr-incorporation in CdO lattice results in a gradual enhancement of certain carrier-compensator like defects such as oxygen interstitials (O_i) in order to keep the charge balance in the system. This results in the reduction of free carrier concentration with higher Cr incorporation levels. Similar explanation was also adopted and examined by X-ray photoelectron spectroscopy in Cr-doped ZnO [13].

The mobility, as shown in fig.4b, varies in complicated manner in such a way that it was sharply increased within a small range of Cr% incorporation level attaining 85.2 $cm^2/V.s$ for CdO:1.2%Cr sample, which is one of the highest value found for doped CdO grown on glass substrate. As known, the scattering of carriers constrains the mobility. The monotonically improvement of crystallinity in between 1% and 1.8% is seems to be mainly responsible for the improvement of mobility. Generally, in the r-interval of 1-1.8%, sample can get high mobility 85.2 $cm^2/V.s$ and conductivity 2150 S/cm. Then**, t**he monotonic and gradual decrease in carrier mobility with increasing Cr incorporation can be attributed to the enhancement of scattering by Cr^{3+} incorporated ions, O_i, accumulated Cr on crystallite (CB) and grain (GB) boundaries, and to the deterioration of crystalline quality of the film that enhance the scattering of free carriers [13,22]. The carrier mean-free-path (mfp) is defined as [23,24]:

$$mfp = \left(h / 2e\right)\left(3N_{el} / \pi\right)^{1/3} \mu \qquad (1)$$

where h is the Planck constant and e is the electronic charge. The Cr-incorporation dependence of mfp is plotted in fig.3 for comparison with mean CS. One can observe identical trade of CS and mfp curves especially for $r \geq 1.8$, which reflects the close relation between CS and mfp. In that range of r, the majority of the incorporated Cr ions accumulated on the crystallite (CB) and grain (GB) boundaries and the electron-CB scattering is predominant one and controls the whole electronic scattering process, thus there is a close relationship between CB and mfp. However, for $r < 1.8$, several competed scattering mechanisms are available: electron-phonon, electron-Cr ion impurity, electron-O_i defects, and electron-CB. For comparison with other investigations, the mobility and conductivity of Cr-doped ZnO are reduced with Cr doping, and that was explained by enhancing of the carrier scattering by Cr ions accumulated on the grain boundaries [25,26].

3.3. Optoelectronic properties

The normal transmittance T(λ) of the prepared Cr-doped CdO films grown on corning glass substrate in the UV-VIS-NIR region (300–3000 nm) are depicted in fig.5. It is clear that the

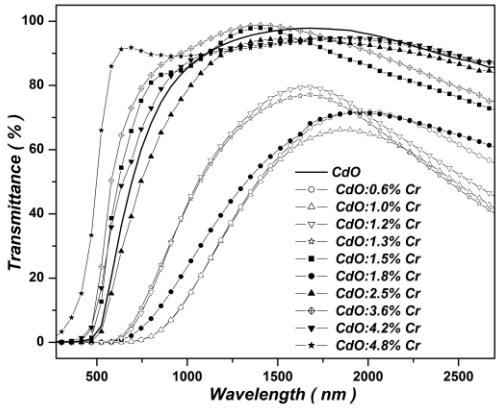

Fig.5 Optical transmittance of the pure and Cr-incorporated CdO films deposited on glass substrates.

maxima (λ_m) of the transmittance T(λ) spectra are in the NIR region; i.e. in the range 1400 □ □2000 nm. In addition, the high-wavelength side of the transmittance curves T(λ) of the doped CdO samples shows a clear damping due to the high density of free electrons [27]. The spectral absorption coefficient α(λ) is related to the absorbance A(λ) by $A(\lambda) = \alpha(\lambda)d$, where d is the film's thickness. The absorbance $A(\lambda)$

can be calculated directly from the experimental data by using the following equation [28]: $A(\lambda) = \ln[1/T]$.The optical band gap E_g is evaluated according to the well-known energy-exponential relation [29]:

$$A\,E = B_{op}\ (E - E_g)^m \qquad (2)$$

where B_{op} is the film's constant and the exponent m is equal to 0.5 or 2 for direct or indirect transitions, respectively. Thus, the extrapolation of the bandgap-plot of $(AE)^2$ *vs. E* for any sample, as shown in fig.6a and fig.6b gives the values of its direct band gap (table 1). The inset of fig.6b shows the Tauc plot for pure Cr_2O_3 film (its XRD is shown in fig. 2b), where the bandgap at 3.57 eV corresponds to spin allowed d-d transitions of Cr^{3+} in octahedral environment [30]. Such bandgap was measured to be 3.5 eV in Ref.[31] or 4.1 eV in Ref.[32]. The lower-energy hump appears in fig.6b is thought to be due to the defects and structural disorder in the amorphous matrix. This bandgap appears in the CdO:Cr samples of higher Cr-incorporation level at 2.85 eV, 3.10 eV, and 3.51 eV for samples CdO:3.6% Cr, CdO:4.2% Cr CdO:4.8% Cr, respectively. Thus the bandgap increases with increasing Cr-incorporation content towards the value 3.57 eV that was found for pure Cr_2O_3 film. This can be explained by increasing of the accumulation of Cr oxide on the crystallite and grain boundaries, which can be detected optically.

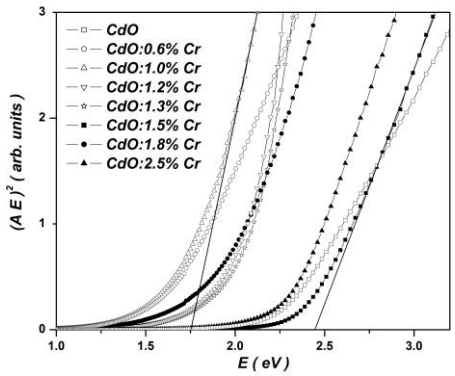

Fig.6a Tauc plot for pure and Cr-incorporated CdO films. The lines determine the direct bandgaps.

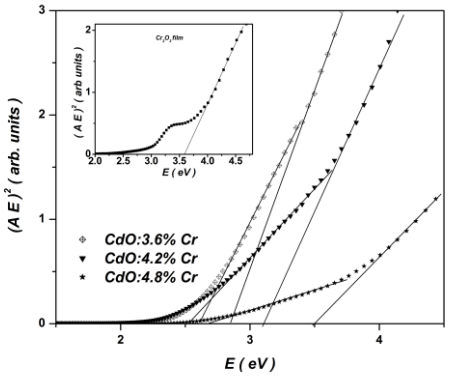

Fig.6b Tauc plot for heavy Cr-incorporated CdO films. The lines determine the direct bandgaps for host CdO and for that Cr oxide accumulated on crystallite and grain boundaries. The inset shows the Tauc plot for pure Cr2O3 film.

For undoped CdO film, the bandgap obtained is in the range (2.2 eV- 2.6 eV) that is known for films prepared by different techniques [2]. The variation of E_g with Cr-incorporation level has two components: the bandgap widening (BGW) [33] and bandgap narrowing (BGN). The bandgap narrowing (BGN) in heavy donor doping may be attributed to the following effects: The doping changes in electron-host ions interaction and introduces electron-ionized impurity interaction, which cause conduction-band renormalization effects and impurity band tailing broadening that finally leads to mergence of the impurity band with the conduction band causing decrease in the effective optical bandgap E_g [34,35].

Phenomenologically, it is possible to correlate the bandgap variations with the carrier concentration by considering both BGW and BGN. The BGW is given by $BGW = S_{BGW}\, N_{el}^{2/3}$ [33], where $S_{BGW}^{th} = 1.348\times10^{-18}$ eV.m^2. The BGN is given by $BGN = (S_{BGN}^{(1)} N_{el}^{2/3} + S_{BGN}^{(2)} N_{el}^{1/3})$, where $S_{BGN}^{(1)} = 4.49\times10^{-19}$ eV.m^2 and $S_{BGN}^{(2)} = 2.836\times10^{-9} / \varepsilon_r$ [10,36]. The effective dielectric constant ε_r can be considered as $\varepsilon_r = \alpha\,\varepsilon_\infty$,where α is a film's parameter that might comes from the non-parabolic band effects and ε_∞ is long-wavelength dielectric constant that equal about $\varepsilon_\infty = n^2 = 1.6^2$ for pure CdO. Thus;

$$\Delta E_g = E_g - E_{g0} = BGW - BGN = S_{BGW,BGN}\, N_{el}^{2/3} - S_{BGN}^{(2)} N_{el}^{1/3} + C_f \qquad (3)$$

where C_f is a fitting parameter and $S_{BGW,BGN} = S_{BGW} - S_{BGN}^{(1)} = 8.98\times10^{-19}\, eV.m^2$. Straight line was obtained by plotting optoelectronic function $OEF = (E_g - S_{BGW,BGN}\, N_{el}^{2/3})$ vs. $N_{el}^{1/3}$, as shown in the inset of fig.4b, with $S_{BGN}^{(2)} = 2.9\times10^{-9}$ eV.m, thus α= 0.4. The experimental and theoretical orders of magnitudes of $S_{BGN}^{(2)}$ are identical.

3.4 Infrared absorption

It is well known that the absorption in the NIR spectral region is mainly caused by the free carriers [37], which can be studied in the framework of classical Drude theory [38]. For the long-wavelength side of T(λ) spectra i.e. for $\lambda > \lambda_m$, the absorption coefficient α is related to the wavelength according to the following relation [37,39]:

$$\alpha = \frac{e^3 N}{4\pi^2 c^3 n \varepsilon_0 m_e^{*2} \mu}\lambda^2 = 5.243\times10^{-13}\frac{N}{n\gamma^2\mu}\lambda^2 \qquad (4)$$

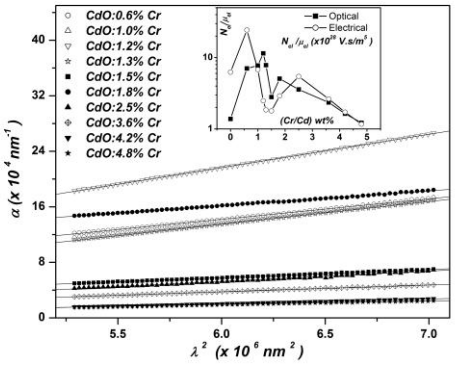

Fig.7 Dependence of absorption coefficient, α on λ^2 in NIR spectral region for Cr-incorporated CdO films. The inset shows the dependence of the (N_{el}/μ) ratio measured optically (op) and electrically (el), on the Cr-incorporation level in CdO films

in mks system where c is the speed of light, n is the refractive index at NIR region (n=1.6), and ε_0 is the permittivity of free space, e, N, and μ are the electronic charge, density, and mobility, respectively. For pure CdO, the reduced effective mass m_e^* is equal to γm_e, where $\gamma = 0.274$ and m_e is the free-electron mass [40]. By neglecting of small variations of n in the NIR, a linear α vs. λ^2 relationship should be observed, as shown in fig.7. Thus, it is possible to estimate the ratio $(N/\mu)_{op}$ (i.e. measured optically) and the results are given in table 1 and fig.7. It is known that Hall measurements are acquired across macroscopic (~0.5 cm)-length scales and thus can potentially be affected by crystallite grain-boundary scattering, if significant. However, optical measurements are much less sensitive to crystallite and grain boundaries as long as carrier mean-free-paths are much smaller than crystallite sizes [5]. But in the present case the restrictions of conduction determinants by induced point defects in the lattice make small difference between electrical and optical method of measuring conduction determinants. Thus, within the experimental error, it was found identical trades of variations of $(N_{el}/\mu_{el})_{el}$ and $(N_{el}/\mu_{el})_{op}$ with Cr-incorporated.

4. Conclusions

The structural, optical, and dc-electrical properties of Cr-doped CdO films grown on glass substrates were investigated. The structure studies show that incorporated Cr ions dissolved into the lattice of CdO and for higher doping level r ≥ 1.8% some of the incorporated Cr ions accumulated on the crystallite and grain boundaries in form of amorphous Cr oxide, which can be discovered by optical absorption and electrical methods. It was concluded that the occupation of interstitial locations of CdO lattice by Cr^{3+} (Cr_i) ions is the most likely to happen. Such type of doping disturbs the charge neutrality of the unit cell that can be settled by creation of Cd^{2+} ion vacancies (V_{Cd}) and/or insertion of interstitial oxygen (O_i). The entered Cr^{3+} ions in CdO lattice behave like donors while the O_i ions behave like carrier-compensator or trap defects. With this conclusive model, one can explain the electrical behavior of Cr-incorporated CdO. The conductivity (σ_{dc}) and carrier concentration (N_{el}) of pure CdO thin film was found to be increased rapidly with 0.6% Cr-incorporation to 2890.2 S/cm and 3.63×10^{20} cm^{-3}, respectively, which implies that the light incorporation of Cr ions act as donors. Then, with increasing of Cr-incorporation both σ_{dc} and N_{el} decrease monotonically, which implies enhancement of carrier-compensator like defects. The mobility varies with Cr-incorporation level in such a way that within a small range of Cr-incorporation level (1-1.8%), the mobility strongly increased attaining 85.2 cm^2/V.s with conductivity of 2150 S/cm, which is one of the highest value found for doped CdO grown on glass substrate. The improvement of the mobility was observed accompanied with improving of crystallinity or reducing of structural scattering including crystallite and grain boundary scattering, which improve the electronic transport roads in crystal. From infrared transparent-conducting-oxide (IR-TCO) point of view, chromium is sufficiently effective for CdO light doping. The structural variations affect the bandgap that was calculated in the framework of available models of simultaneous bandgap widening and narrowing. The utmost improvement of conduction determinants takes place with CdO:1.3wt% Cr sample, so that the conductivity increases by about 43 times, mobility by about 12 times, and electronic concentration by about 3.5 times compare with undoped CdO film prepared by the same method.

Table 1. The measured electrical parameters [resistivity (ρ), mobility (μ_{el}), and carrier concentration (N_{el})], bandgap (E_g) for pure and Cr-incorporated CdO films grown on glass substrate. The ratio (N_{el}/μ_{el}) measured electrically (el) and optically (op) are given in units ($\times 10^{28}$ V.s/m^5)

Sample	ρ □ $\times 10^{-4}$ Ω□cm)	μ_{el} □ □cm^2/V.s)	$N_{el}(10^{20}$ $cm^{-3})$	E_g (eV)	$(N_{el}/\mu_{el})_{el}$	$(N_{el}/\mu_{el})_{op}$
CdO	201	7.03	0.44	2.3	6.25	1.38
CdO:0.6%Cr	3.46	27.2	6.63	1.61	24.37	7.04
CdO:1.0%Cr	5.82	39.7	2.7	1.75	6.80	7.73
CdO:1.2%Cr	8.14	47.7	1.61	2.05	2.49	11.48
CdO:1.3%Cr	4.65	**85.2**	1.58	2.03	1.85	7.85
CdO:1.5%Cr	7.78	66.78	1.2	2.4	1.79	2.8
CdO:1.8%Cr	12.7	41.2	1.2	1.95	2.91	5.07
CdO:2.5%Cr	17.05	25.91	1.414	2.28	5.45	3.58
CdO:3.6%Cr	38.3	24.86	0.656	2.62	2.63	2.35
CdO:4.2%Cr	84.47	14.35	0.515	2.52	1.72	1.64
CdO:4.8%Cr	87.22	24.75	0.289	2.7	1.16	1.22

References

[1] S. Calnan, A. N. Tiwari, thin solid Films 518 (2010) 1839.
[2] Z. Zhao, D. L. Morel, C. S. Ferekides, Thin Solid Films 413 (2002) 203.
[3] D. M. Carballeda-Galicia, R. Castanedo-Perez, O. Jimenez-Sandoval, S. Jimenez-Sandoval, G. Torres-Delgado, C. I. Zuniga-Romero,Thin Solid Films 371 (2000) 105.
[4] M. Burbano, D. O. Scanlon, G. W. Watson, J. Am. Chem. Soc. 133 (2011) 15065.
[5] A. W. Metz, J. R. Ireland, J. –G. Zheng, R. P. S. M. Lobo, Yu Yang, Jun Ni, C. L. Stern, V. P. Dravid, N. Bontemps, C. R. Kannewurf, K. R. Poeppelmeier, T. J. Marks, J Am Chem Soc. 126 (2004) 8477.

[6] T. J. Coutts, D. L. Young, X. Li, W. P. Mulligan, X. Wu, J. Vac. Sci. Technol. A 18 (2000) 2646.
[7] Y. Dou, R. G. Egdell, T. Walker, D. S. L. Law, G. Beamson, Surface Science 398 (1998) 241.
[8] A. A. Dakhel, Phys. Stat. Sol. (a) 205 (2008) 2704.
[9] R. K. Gupta, K. Ghosh, R. Patel, S. R. Mishra, P. K. Kahol, Curr. Appl. Phys. 9 (2009) 673.
[10] A. A. Dakhel, Thin Solid Films 518 (2010) 1712.
[11] L. Li, H. Liu, X. Luo, X. Zhang, W. Wang, Y. Cheng, Q. Song, Solid State Communications 146 (2008) 420
[12] K. Sato, H. Katayama-Yoshida, *Semicond. Sci. Technol.* 17 (2002) 367.
[13] R. S. Ajimsha, A. K. Das, B. N. Singh, P. Misra, L. M. Kukreja, Physica B 406 (2011) 4578.
[14] S. –J. Liua, L. –Y. Chen, C. –Y. Liu, H. –W. Fang, J. –H. Hsieh, J. –Y. Juang, Appl. Surf. Sci. 257 (2011) 2254.
[15] D. N. Chavan, G. E. Patil, D. D. Kajale, V. B. Gaikwad, G. H. Jain, Sensors & Transducers J. 125 (2011)142.
[16] L. San-Bing, L. Jun-Qian, Chinese J. Struct. Chem, 28 (2009) 360.
[17] J. M. Jaklevic, F. S. Goulding, "Energy Dispersion" in "X-ray Spectrometry" H. K. Herglotz, L. S.Birks (eds.), P.50, NY: M. Dekker, 1978.
[18] Powder Diffraction File, Joint Committee for Powder Diffraction Studies (JCPDS) file No. 05-0640.
[19] Powder Diffraction File, Joint Committee for Powder Diffraction Studies (JCPDS) file No. 38-1479.
[20] R. D. Shannon, Acta Crystallographica A 32 (1976) 751.
[21] J. I. Langford, A. J. C. Wilson, J. Appl. Cryst. 11(1978) 102.
[22] S. Shu, Y. Yang, J. E. Medvedova, J. R. Ireland, A. W. Metz, J. Ni, C. R. Kannewurf, A. J. Freeman , T. J. Tobin, J. American Chem. Soc. 126 (2004) 13787.
[23] M. Chen, Z. L. Pei, X. Wang, Y. H. Yu, X. H. Liu, C. Sun, L. S. Wen, J. Phys. D: Appl. Phys. 33 (2000**)** 2538.
[24] D. H. Zhang, H. L. Ma, Appl. Phys. A 62 (1996) 487.
[25] S. Singh, E. S. Kumar,M. S. R. Rao, Scripta Materialia 58 (2008) 866.
[26] K. Tominaga, T. Takaoa, A. Fukushima, T. Morigab, I. Nakabayashib, Vacuum 66 (2002) 511.
[27] A. A. Dakhel, Mater. Chem. Phys. 117 (2009) 284.
[28] W. Q. Hong, J. Phys. D: Appl. Phys. 22 (1989) 1384.
[29] J. Tauc, F. Abelesn (ed.), Optical Properties of Solids. North Holland,1969.
[30] S. Hong, E. Kim, D. –W. Kim, T. –H. Sung, K. No, J. Non-Cryst. Solids 221 (1997) 245
[31] R. E. Kirby, E. L. Garwin, F. K. King, A. R. Nyaiesh, J. Appl. Phys. 62 (1987) 1400.
[32] T. I. Y. Allos, R. R. Birss, M. R. Parker, E. Ellis, D.W. Johnson, Solid State Commun. 24 (1977) 129.
[33] J. I. Pankove, Optical Processes in Semiconductors, P.36, Dover, NY, 1975.
[34] Y. Z. Zhang, J. G. Lu, Z. Z. Ye, H. P. He, L. P. Zhu, B. H. Zhao, L. Wang, Applied Surface Science 254 (2008) 1993.
[35] W. Walukiewicz, Phys. Rev. B 41 (1990) 10218.
[36] A. A. Dakhel, Curr. Appl. Phys. 11 (2011) 11.
[37] Z. Qiao, C. Agashe, D. Mergel, Thin Solid Films 496 (2006) 520.
[38] D. Mergel, Z. Qiao, J. Phys. D: Appl. Phys. 35 (2002) 794.
[39] A. A. Dakhel, Solar Energy 84 (2010) 1433.
[40] R. Asahi, A. Wang, J. R. Babcock, N. L. Edleman, W. Metza, M. A. Lane, V. P. Dravid, C. R. Kannewurf, A. J. Freeman, T. J. Marks, Proceeding of the Int. symposium on transparent oxide thin films for electronics and optics, Nov. 8-9, 2001, Tokyo, Japan.